Stability of axisymmetric Taylor-Couette flow in hydromagnetics

Günther Rüdiger*

Astrophysikalisches Institut Potsdam, An der Sternwarte 16, D-14482 Potsdam, Germany

Dima Shalybkov[†]

A.F. Ioffe Institute for Physics and Technology, 194021, St. Petersburg, Russia

The linear marginal instability of an axisymmetric magnetohydrodynamics Taylor-Couette flow of infinite vertical extension is considered. We are only interested in those vertical wave numbers for which the characteristic Reynolds number is minimum. For hydrodynamically unstable flows minimum Reynolds numbers exist even without a magnetic field, but there are also solutions with *smaller* characteristic Reynolds numbers for certain weak magnetic fields. The magnetic field, therefore, destabilizes the rotating flow by the so-called magnetorotational instability (MRI). The MRI, however, can only exist for hydrodynamically unstable flow if the magnetic Prandtl number, Pr, is not too small. For too small magnetic Prandtl numbers (and too strong magnetic fields) only the well-known magnetic suppression of the Taylor-Couette instability can be found. The MRI is even more pronounced for *hydrodynamically stable* flows. In this case we can always find a magnetic field amplitude where the characteristic Reynolds number is minimum. These critical values are computed for different magnetic Prandtl numbers and for three types of geometry (small, medium, and wide gaps between the rotating cylinders). In all cases the minimum Reynolds numbers are running with 1/Pr for small enough Pr so that the critical Reynolds numbers may easily exceed values of 10^6 for the magnetic Prandtl number of sodium (10^{-5}) or gallium (10^{-6}). The container walls are considered either electrically conducting or insulating. For insulating walls with small and medium-size gaps between the cylinders (i) the critical Reynolds number is smaller, (ii) the critical Hartmann number is higher, and (iii) the Taylor vortices are longer in the direction of the rotation axis. For wider gaps the differences in the results between both sets of boundary conditions become smaller and smaller.

I. INTRODUCTION

The longstanding problem of the generation of turbulence in various hydrodynamically stable situations has found a solution in recent years with the so-called magnetorotational instability (MRI), also referred to as the Balbus-Hawley instability, in which the presence of a magnetic field has a destabilizing effect on a differentially rotating flow, provided that the angular velocity decreases outwards with the radius. This MRI has been discovered decades ago [1,2] for ideal Couette flow, but its importance as the source of turbulence in accretion disks with differential (Keplerian) rotation was only recognized by Balbus and Hawley [3].

However, the MRI has never been observed in laboratory [4–7]. Moreover, Chandrasekhar [2] already suggested the existence of the MRI for ideal Taylor-Couette flow, but his results for nonideal fluids for small gaps and within the small magnetic Prandtl number approximation demonstrated the absence of the MRI for hydrodynamically unstable flow. Recently, Goodman and co-workers [8,9] claimed that this absence of MRI was due to the use of the small magnetic Prandtl number limit. The magnetic Prandtl number is really very small under laboratory conditions ($\sim 10^{-5}$ and smaller). Obviously, a proper understanding of this phenomenon is very important for possible future experiments, including Taylor-Couette flow dynamo experiments. The dependence of a real Couette flow on magnetic Prandtl number and gap width between rotating cylinders is investigated. The simple model of uniform density fluid contained between two vertically infinite rotating cylinders is used with constant magnetic field parallel to the rotation axis (Fig. 1). The unperturbed state is any stationary circular flow of an incompressible fluid. In the absence of viscosity, the class of such flows is very wide: indeed, if Ω denotes the angular velocity of rotation about the axis, then the equations of motion allow Ω to be an arbitrary function of the distance R from the axis, provided the velocities in the radial and the axial directions are zero. For viscous flows, however, the class becomes very restricted: in fact, in the absence of any transverse pressure gradient, the most general form of Ω allowed is

$$\Omega(r) = a + b/R^2, \tag{1}$$

where a and b are two constants related to the angular velocities Ω_{in} and Ω_{out} with which the inner and the outer cylinders are rotating. If R_{in} and R_{out} ($R_{out} > R_{in}$) are the radii of the two cylinders then

$$a = \Omega_{in} \frac{\hat{\mu} - \hat{\eta}^2}{1 - \hat{\eta}^2} \quad \text{and} \quad b = \Omega_{in} R_{in}^2 \frac{1 - \hat{\mu}}{1 - \hat{\eta}^2} \tag{2}$$

with

———————
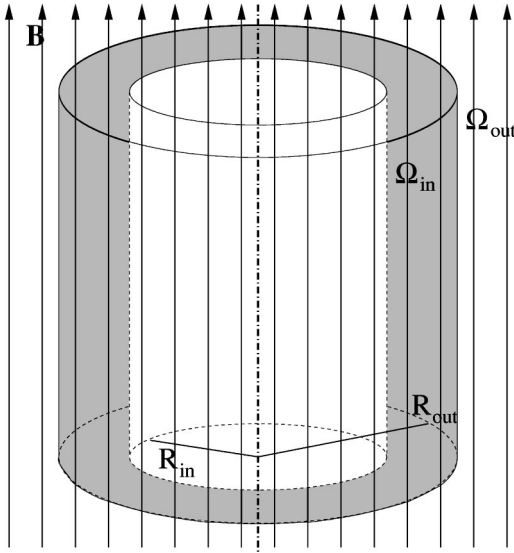*Electronic address: gruediger@aip.de

[†]Electronic address: dasha@astro.ioffe.rssi.ru

FIG. 1. Cylinder geometry of the Taylor-Couette flow.

$$\hat{\mu} = \Omega_{out}/\Omega_{in} \quad \text{and} \quad \hat{\eta} = R_{in}/R_{out}. \quad (3)$$

Following the Rayleigh stability criterion, $d(R^2\Omega)^2/dR > 0$, rotation laws are hydrodynamically stable for $\hat{\mu} > \hat{\eta}^2$. Taylor-Couette flows with outer cylinders at rest ($\hat{\mu} = 0$) are thus never stable.

Here, in order to isolate the MRI we are mainly interested in flows with rotating outer cylinders so that the hydrodynamic-stability criterion, $\hat{\mu} > \hat{\eta}^2$, is fulfilled. Our reference case is $\hat{\eta} = 0.5$ and $\hat{\mu} = 0.33$.

II. BASIC EQUATIONS

R, ϕ, and z are the cylindrical coordinates. A viscous electrically conducting incompressible fluid between two rotating infinite cylinders in the presence of a uniform magnetic field parallel to the rotation axis admits the basic solution $U_R = U_z = B_R = B_\phi = 0$ and

$$B_z = B_0 = \text{const}, \quad U_\phi = aR + b/R, \quad (4)$$

with U the velocity and B the magnetic field, a and b are given by Eq. (2). We are interested in the stability of this solution. The perturbed state of the flow may be described by

$$u_R, U_\phi + u_\phi, u_z, b_R, b_\phi, B_0 + b_z, \delta P \quad (5)$$

with δP as the pressure perturbation.

The linear stability problem is considered with only axisymmetric perturbations. By analyzing the disturbances into normal modes the solutions of the linearized magnetohydrodynamical equations are of the form

$$u_R = u_R(R)e^{\omega t}\cos(kz), \quad b_R = b_R(R)e^{\omega t}\sin(kz),$$

$$u_\phi = u_\phi(R)e^{\omega t}\cos(kz), \quad b_\phi = b_\phi(R)e^{\omega t}\sin(kz),$$

$$u_z = u_z(R)e^{\omega t}\sin(kz), \quad b_z = b_z(R)e^{\omega t}\cos(kz). \quad (6)$$

Stationary modes are always easier to excite than oscillatory ones [2,10]. So, only marginal stability will be considered ($\omega = 0$). The derivation of the equations describing this situation is due to Chandrasekhar [2]; it should not be repeated here. We only use a different normalization here. Let $d = R_{out} - R_{in}$ be the gap between the cylinders. We use

$$H = (R_{in}d)^{1/2} \quad (7)$$

as unit of length, the Alfvén velocity $V_A = B_0/(\mu_0\rho)^{1/2}$ as unit of perturbed velocity, and $B_0 Pr^{1/2}$ as unit of perturbed magnetic field with the magnetic Prandtl number

$$Pr = \frac{\nu}{\eta}, \quad (8)$$

ν is the kinematic viscosity, η is the magnetic diffusivity. Note that wave numbers are given in units of H^{-1}.

Using the same symbols for normalized quantities as before, the equations take the form

$$(DD_* - k^2)^2 u_R + k^2 Ha^2 u_R - 2k^2 Re\frac{\Omega}{\Omega_{in}}u_\phi = 0,$$

$$(DD_* - k^2)u_\phi + kHa\, b_\phi - Re\frac{1}{R}\frac{d}{dR}\left(R^2\frac{\Omega}{\Omega_{in}}\right)u_R = 0,$$

$$(DD_* - k^2)b_R - kHa\, u_R = 0,$$

$$(DD_* - k^2)b_\phi - kHa\, u_\phi + Re\, Pr R\frac{d}{dR}\left(\frac{\Omega}{\Omega_{in}}\right)b_R = 0, \quad (9)$$

with

$$Ha = \frac{B_0 H}{\sqrt{\mu_0\rho\nu\eta}}, \quad Re = \frac{\Omega_{in}H^2}{\nu}, \quad (10)$$

where Ha is the Hartmann number, Re is the Reynolds number of the inner rotation, ρ is the density, μ_0 is the magnetic constant. Chandrasekhar's notations $D = d/dR$ and $D_* = d/dR + 1/R$ are also used.

Let us emphasize that Pr appears only once in the fourth equation of the system (9). Recall that under terrestrial conditions Pr is small ($\sim 10^{-5}$ and smaller). If the approximation Pr=0 is adopted, the governing tenth-order system (9) can be factorized into an eighth-order system, which does not involve b_R, and a second-order system for b_R [the third equation of the system (9)]. This fact was recognized by Chandrasekhar [2] for the case of a narrow gap; but it is true also in the case of a finite gap. An appropriate set of ten boundary conditions is needed to solve the system (9). The situation is more difficult than in the small-gap-small-Prandtl-number case where only eight boundary conditions are needed. No-slip conditions for the velocity on the walls are used throughout, i.e.,

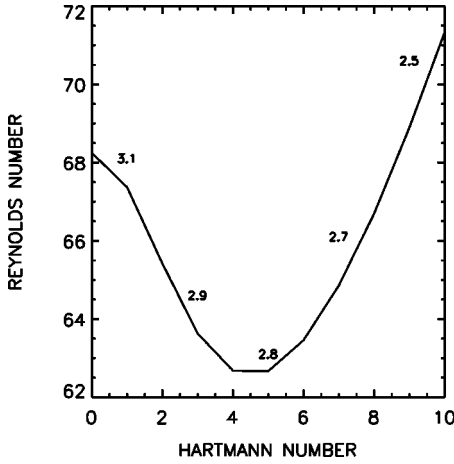$$u_R = 0, \quad u_\phi = 0, \quad \frac{du_R}{dR} = 0, \quad (11)$$

FIG. 2. The stability line for Taylor-Couette flow with outer cylinder at rest for $\hat{\eta}=0.5$ and Pr$=1$. The flow is unstable above the line. There is instability even without magnetic fields but its excitation is easier with magnetic fields with Ha $\simeq 4.5$. The line is marked with those wave numbers for which the Reynolds numbers are minimum.

(see [2]). The magnetic boundary conditions depend on the electrical properties of the walls. The transverse currents and perpendicular component of magnetic field should vanish on conducting walls, hence

$$\frac{db_\phi}{dR}+\frac{b_\phi}{R}=0,\quad b_R=0. \tag{12}$$

The above boundary conditions (11) and (12) are valid for $R=R_{\text{in}}$ and for $R=R_{\text{out}}$.

The situation changes for insulating walls. The magnetic field must match the external magnetic field for nonconducting walls. The boundary conditions are different at $R=R_{\text{in}}$ and at $R=R_{\text{out}}$ due to the different behavior of the modified Bessel functions for $R\to 0$ and $R\to\infty$, i.e.,

$$b_\phi=0,\quad \frac{\partial}{\partial R}(Rb_R)=b_R\frac{kRI_0(kR)}{I_1(kR)} \tag{13}$$

for $R=R_{\text{in}}$ and

$$b_\phi=0,\quad \frac{\partial}{\partial R}(Rb_R)=-b_R\frac{kRK_0(kR)}{K_1(kR)} \tag{14}$$

for $R=R_{\text{out}}$ where I_n and K_n are the modified Bessel functions (cf. [9]).

The homogeneous set of equations (9) with boundary conditions either Eqs. (11) and (12) for conducting walls or Eqs. (11), (13), and (14) for insulating walls determine the eigenvalue problem of the form $L(\hat{\mu},\hat{\eta},k,\text{Pr},\text{Re},\text{Ha})=0$. System (9) was approximated by finite differences. The typical number of grid points used in calculations was 200. The resulting determinant, L, takes the value zero if and only if the values Re are the eigenvalues. Since the determinant changes sign on passing through a zero, an automatic search routine may be employed to locate these zeros. For given values $\hat{\mu}$, $\hat{\eta}$, Pr,
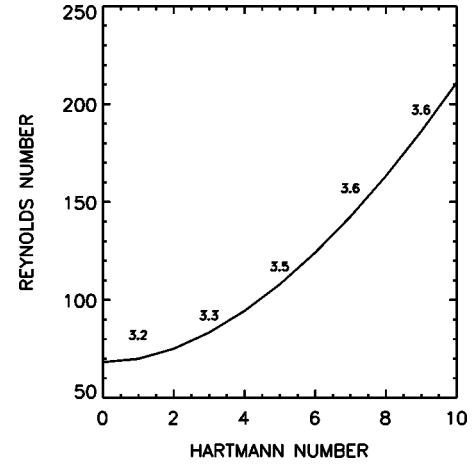

FIG. 3. The same as in Fig. 2 but for Pr$=10^{-5}$. The minimum for Pr$=1$ has now disappeared completely.

Ha, which determine the basic velocity state and magnetic field strength, we seek the minimum real positive Re over real $k\geq 0$ for which there is a solution for $L=0$.

III. RESULTS FOR CONDUCTING WALLS

We start with the results for containers with conducting walls and outer cylinders at rest but with various gap sizes (medium, wide, and small). In all these cases there are linear instabilities even without magnetic fields. We are here concerned with the influence of the magnetic field. If the resulting eigenvalue with magnetic field exceeds the eigenvalue without magnetic field then we have only the well-known effect of magnetic stabilization rather than magnetic destabilization. As we shall see, this is indeed the case for sufficiently small magnetic Prandtl numbers.

A. Outer cylinder at rest

In Fig. 2 an outer cylinder at rest is considered ($\hat{\mu}=0$) for a medium-size gap of $\hat{\eta}=0.5$ and for Pr$=1$. As we know for vanishing magnetic field and for $\hat{\eta}=0.5$ the exact Reynolds number for this case is 68.2 (see [2])—well represented by the result for Ha$=0$ in Fig. 2. But for increasing magnetic field the Reynolds number is reduced so that the excitation of the Taylor vortices becomes easier than without magnetic field. The minimum Reynolds number Re$_{\text{crit}}$ of about 63 for Pr$=1$ is reached for Ha$_{\text{crit}}\simeq 4$–5. This magnetically induced subcritical excitation of Taylor vortices is due to the MRI. We shall always refer to the minimum Reynolds number as the critical Reynolds number and the corresponding Hartmann number as critical Hartmann number.

For stronger magnetic fields, the instability is suppressed by the magnetic field—as it must be—so that the Reynolds number grows without bounds. In Fig. 3 the same container is considered but for a small magnetic Prandtl number of 10^{-5}. The minimum, which is well pronounced for Pr$=1$ case, disappears completely. A suppression of the instability by the magnetic field can only be observed.
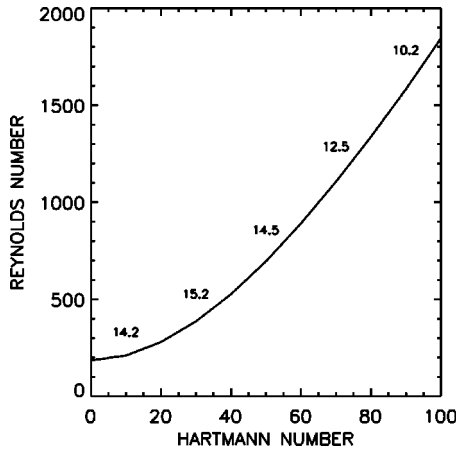
FIG. 4. The stability line for the flow in a small gap ($\hat{\eta}$ =0.95) with an outer cylinder at rest and for Pr=10^{-5}.

The results for small and wide gaps between the cylinders are presented in Fig. 4 and Table I. The situation is analogous to the medium-size gap. The magnetic suppression of the Taylor-Couette flow instability is only observed for small Pr.

TABLE I. Conducting walls: Minimum Reynolds numbers and related wave numbers for a flow with outer cylinder at rest ($\hat{\mu}$ =0).

| $\hat{\eta}$	Pr	Ha	Re	k
0.25	10^{-5}	0.0	78.8	1.9
0.25	10^{-5}	1.0	84.4	1.9
0.25	10^{-5}	2.0	100.	2.0
0.25	10^{-5}	4.0	157.	2.1
0.25	10^{-5}	6.0	243.	2.3
0.25	10^{-5}	8.0	350.	2.5
0.25	10^{-5}	10.0	475.	2.7
0.25	1	0.0	78.8	1.9
0.25	1	1.0	71.4	1.8
0.25	1	2.0	62.1	1.7
0.25	1	4.0	57.7	1.6
0.25	1	6.0	61.9	1.5
0.25	1	8.0	68.7	1.4
0.25	1	10.0	76.6	1.3
0.95	1	0.0	185	13.6
0.95	1	10	190	13.3
0.95	1	20	203	12.6
0.95	1	40	248	10.9
0.95	1	60	303	10.5
0.95	1	80	362	8.4
0.95	1	100	423	7.6
0.95	2	0.0	185	13.6
0.95	2	10	173	12.8
0.95	2	20	166	12.0
0.95	2	40	185	10.6
0.95	2	60	220	9.4
0.95	2	80	261	8.4
0.95	2	100	303	7.6
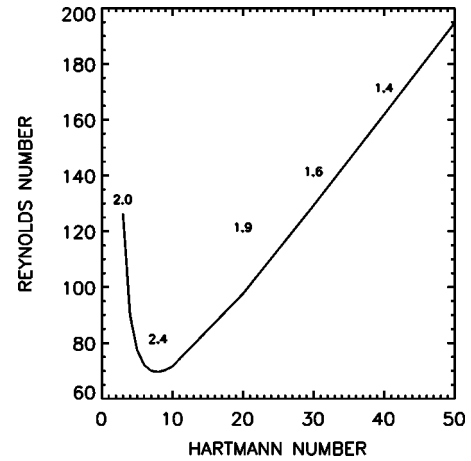
FIG. 5. The stability line for $\hat{\eta}$=0.5 and Pr=1. The outer cylinder rotates with 33% of the rotation rate of the inner cylinder so that, from the Rayleigh criterion, the hydrodynamic instability for Ha=0 disappears. The minimum Reynolds number is almost the same as in Fig. 2.

This is the reason why Chandrasekhar did not find the MRI in his detailed numerical calculations for small gaps and very small magnetic Prandtl numbers. Figure 4 shows the result for the small-gap-small-Prandtl approximation used by Chandrasekhar [2]. Obviously, the MRI does not work efficiently in the limit of small magnetic Prandtl numbers, i.e., for too low electrical conductivity.

In order to find a minimum due to the MRI the magnetic Prandtl number must exceed some critical value, Pr$_{\min}$, for hydrodynamically unstable flow ($\hat{\mu} < \hat{\eta}^2$). The critical Prandtl number can be calculated by

$$\mathrm{Pr}_{\min}=0.25+1.5\hat{\eta}^2-0.75\hat{\mu}^2. \quad (15)$$

This expression provides reasonable accuracy of about 30% for all calculated cases (more than presented here). The critical magnetic Prandtl numbers lie in the narrow interval 0.25 . . . 1.75 for any $\hat{\mu}$ and $\hat{\eta}$. Thus, if the electrical conductivity is so small as it is for sodium or gallium then the MRI cannot be observed by corresponding experiments with hydrodynamically unstable flows.

B. Rotating outer cylinder

Another situation occurs if the outer cylinder rotates so fast that the rotation law no longer fulfills the Rayleigh criterion, and a solution for Ha=0 cannot exist. Then the nonmagnetic eigenvalue along the vertical axis moves to infinity and we should always have a minimum. This is the basic situation in astrophysical applications such as accretion disks with a Kepler rotation law. The main question is whether the critical Reynolds number and the critical Hartmann number can be realized experimentally. The Figs. 5, 6, and Table II present the results for both various Hartmann numbers and magnetic Prandtl numbers for a medium-sized gap of $\hat{\eta}$ =0.5. There are always minima of the characteristic Reynolds numbers for certain Hartmann numbers. The minima and the critical Hartmann numbers increase for decreasing
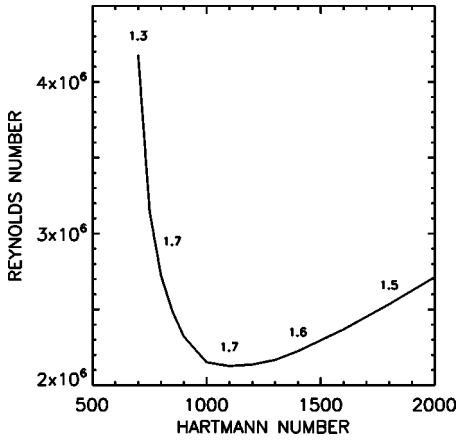
FIG. 6. The same as in Fig. 5 but for $Pr = 10^{-5}$.

magnetic Prandtl numbers. For $\hat{\eta} = 0.5$ and $\hat{\mu} = 0.33$ the critical Reynolds numbers together with the critical Hartmann numbers are plotted in Fig. 7. For the small magnetic Prandtl numbers we find rather simple relations. With

$$Rm = Pr\,Re, \qquad (16)$$

and

$$Ha^* = \sqrt{Pr}\,Ha, \qquad (17)$$

it follows

$$Rm \simeq 21, \qquad (18)$$

and

$$Ha^* \simeq 3.5. \qquad (19)$$

Rm is the magnetic Reynolds number, $Rm = \Omega_{in}H^2/\eta$ (or dynamo number) and Ha* is the Lundquist number $Ha^* = BH/\eta\sqrt{\mu_0\rho}$. For small Pr both quantities do not depend on the microscopic viscosity. Both the minimum magnetic

TABLE II. Conducting walls: Minimum Reynolds numbers and related wave numbers for flow with rotating outer cylinder ($\hat{\mu} = 0.33$) and medium-sized gap ($\hat{\eta} = 0.5$)

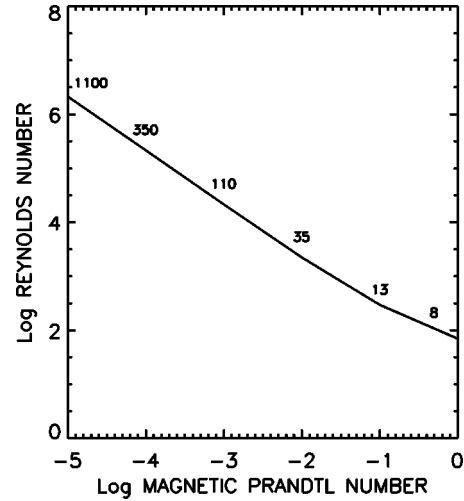| Pr	Ha	Re	k
10^{-4}	200	8.53×10^5	1.0
10^{-4}	300	2.19×10^5	1.7
10^{-4}	350	2.15×10^5	1.7
10^{-4}	400	2.17×10^5	1.7
10^{-4}	500	2.38×10^5	1.6
10^{-2}	20	8.99×10^3	1.0
10^{-2}	25	2.96×10^3	1.6
10^{-2}	30	2.32×10^3	1.7
10^{-2}	35	2.22×10^3	1.8
10^{-2}	50	2.44×10^3	1.6
10^{-2}	70	2.99×10^3	1.5
10^{-2}	100	3.92×10^3	1.3

FIG. 7. The main results for $\hat{\eta} = 0.5$ and $\hat{\mu} = 0.33$: The critical Reynolds numbers for given magnetic Prandtl numbers marked with those Hartmann numbers where the Reynolds number is minimum.

Reynolds number and the corresponding characteristic Lundquist number are thus independent of the value of the kinematic microscopic viscosity.

C. Wide gap

Let us now vary the size of the gap. In view of the experimental possibilities, we shall only work for conducting fluids with the magnetic Prandtl number of sodium, i.e., 10^{-5}. In the present section cylinders with a gap with $\hat{\eta} = 0.25$ are discussed. The outer cylinder is either at rest (Table I) or it is rotating with a frequency satisfying the Rayleigh criterion for stability (Fig. 8). In the first case, of course, there is a solution without magnetic field, i.e., for $Ha = 0$. The corresponding Reynolds number is 78.8. Note again that a minimum appears for $Pr = 1$ which, however, does not survive the decrease of the magnetic Prandtl number to realistic small values.
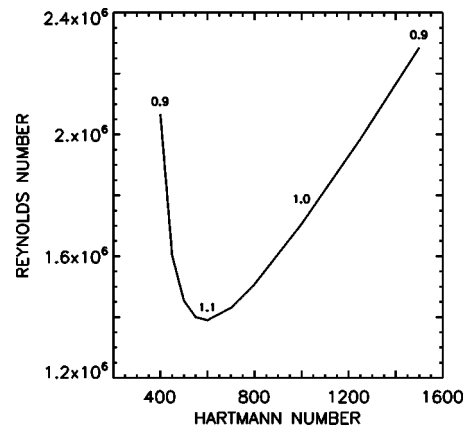

FIG. 8. The stability line for wide gap ($\hat{\eta} = 0.25$), $Pr = 10^{-5}$, $\hat{\mu} = 0.1$.

For experiments with a hydrodynamically stable flow ($\hat{\mu} > \hat{\eta}^2$), the minimum always exists (e.g., for $\hat{\mu} = 0.1$, see Fig. 8). The resulting critical Reynolds number is 1.4×10^6 and the critical Hartmann number is about 600. Let us turn to first estimates. With $\nu = 10^{-2}$ cm^2/s the frequency f of the inner cylinder is

$$f = \frac{1.6 \times 10^{-5} \text{Re}}{\hat{\eta}(1 - \hat{\eta})} \left(\frac{10 \text{ cm}}{R_{\text{out}}} \right)^2 \text{ Hz}, \qquad (20)$$

so that

$$f = \frac{120}{(R_{\text{out}}/10 \text{ cm})^2} \text{ Hz} \qquad (21)$$

corresponding to the frequency of about 19 Hz for a container with an outer radius of 25 cm [11].

For a Hartmann number with the density of liquid sodium ($\rho \simeq 1$ g/cm^3) one finds

$$\text{Ha} = 282 \left(\frac{B}{\text{Gauss}} \right) \left(\frac{R_{\text{out}}}{10 \text{ cm}} \right) \sqrt{\hat{\eta}(1 - \hat{\eta})\text{Pr}}, \qquad (22)$$

hence for $\hat{\eta} = 0.25$ and Pr $= 10^{-5}$,

$$\text{Ha} = 0.39 \left(\frac{B}{\text{Gauss}} \right) \left(\frac{R_{\text{out}}}{10 \text{ cm}} \right). \qquad (23)$$

For a container of (say) 25 cm a field of 500 Gauss yields a Hartmann number of 500. Thus, it is not a problem to reach Hartmann numbers of order 10^4 with the standard laboratory equipment. Note that the Hartmann number is maximum for the experiment with $\hat{\eta} = 0.5$.

We have to realize that there is only suppression of the instability by the magnetic field for Pr $= 10^{-5}$ and hydrodynamically unstable flow (Table I). There is no minimum of the Reynolds number due to the MRI instability. This effect is a consequence of the low magnetic Prandtl number. As it must, the instability disappears for Ha $= 0$ and $\hat{\eta} = 0.25$ if $\hat{\mu} = 0.1$ (Fig. 8). However, we find the instability again for a finite Hartmann number. For Ha ≈ 500 an instability occurs for a Reynolds number of about 10^6. For example, an experiment with a Reynolds number of 1.5×10^6 and an increasing magnetic field should yield the MRI instability between two known very sharp limits [12,13]. The rotation frequency of the inner cylinder must fulfill the above relation (21), i.e., a container with an outer radius of 31 cm must rotate with a frequency of about 10 Hz (see [14]).

D. Small gap

For small gaps and outer cylinder at rest there is no minimum due to the MRI for magnetic Prandtl numbers equal or smaller than Pr$_{\text{crit}}$, but it exists for Pm $>$ Pm$_{\text{crit}}$, where Pr$_{\text{crit}}$ is given by Eq. (15). If the outer cylinder rotates so fast that the hydrodynamic instability disappears the minimum again appears due to the MRI (Fig. 9). However, the Reynolds numbers are far too high for a technical realization (inner
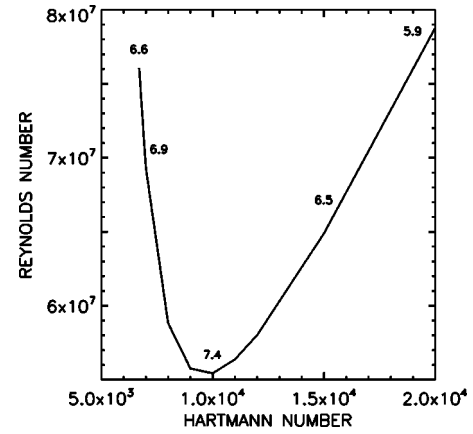

FIG. 9. Small gap ($\hat{\eta} = 0.95$): The same as in Fig. 4 but for a rotating outer cylinder with $\hat{\mu} = 0.95$, Pr $= 10^{-5}$. The critical Reynolds number is extremely high.

rotation frequency is of order 10^3 Hz). Obviously, magnetohydrodynamics Taylor-Couette flows with too small gaps between the cylinders are not suitable for experimental work.

IV. RESULTS FOR INSULATING WALLS

For the sake of completeness containers with insulating walls must be considered. The (complicated) boundary conditions are then given by the relations (13) and (14). Surprisingly, the basic differences can already be demonstrated by the simplest model given in Fig. 10 for the outer cylinder at rest and Pr $= 1$ (see Fig. 2 for comparison). Of course, the curve starts with the same Reynolds number for Ha $= 0$. The minimum, however, is deeper than in Fig. 2 and the corresponding Hartmann number is higher. Note that the vertical wavelength in the minimum is *larger* than in containers with conducting walls. We check these findings under the restriction of small magnetic Prandtl number (10^{-5}) and for rotating outer cylinders for small (Fig. 11), medium (Fig. 12), and wide (Fig. 13) gaps and for the outer cylinder at rest (Table III). The results must be compared with the results given in Figs. 6, 8, 9, and Table I valid for conducting walls. For
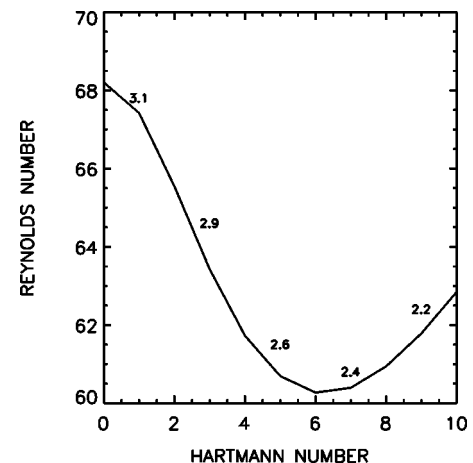

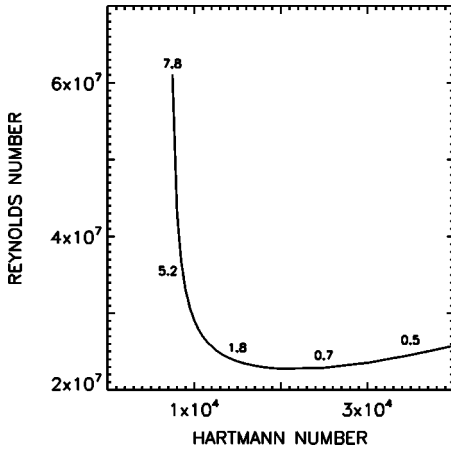FIG. 10. The same as in Fig. 2, but for insulating walls.

FIG. 11. Small gap ($\hat{\eta}=0.95$): The same as in Fig. 9, but for a rotating outer cylinder ($\hat{\mu}=0.95$) embedded in a vacuum. Pr $=10^{-5}$.

small and medium gaps one finds indeed that (i) the minimum Reynolds numbers are smaller, (ii) the corresponding Hartmann number is higher, and (iii) vertical wave number is smaller (i.e., the cells of Taylor vortices are vertically more elongated) for the container with insulating walls. For wide gaps the critical Reynolds number is slightly higher for the container with nonconducting walls, but the vertical size of the cell is practically the same.

V. VERTICAL CELL STRUCTURE

The unstable Taylor-Couette flow forms Taylor vortices. With our normalizations the vertical extent δz of a Taylor vortex is given by

$$\frac{\delta z}{R_{\text{out}}-R_{\text{in}}}=\frac{\pi}{k}\sqrt{\frac{\hat{\eta}}{1-\hat{\eta}}}. \quad (24)$$

The dimensionless vertical wave number k is given in all of the above figures.

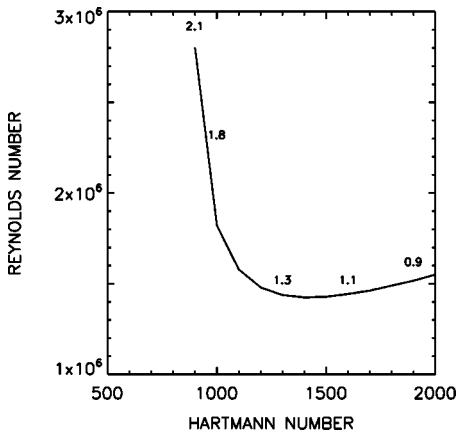

FIG. 12. Medium-size gap ($\hat{\eta}=0.5$): The same as in Fig. 6 but for the rotating outer cylinder ($\hat{\mu}=0.33$) embedded in a vacuum. Pr$=10^{-5}$.
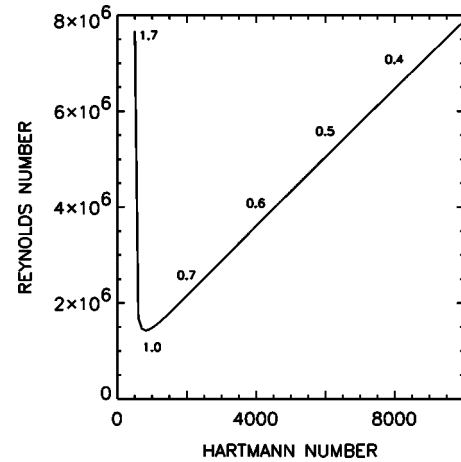

FIG. 13. Wide gap ($\hat{\eta}=0.25$): The same as in Fig. 8 but for the rotating outer cylinder ($\hat{\mu}=0.1$) embedded in a vacuum. Pr $=10^{-5}$.

In the case of hydrodynamically unstable flows we have $\delta z \simeq R_{\text{out}}-R_{\text{in}}$ for small magnetic field (Ha≈ 0) independently of gap size and boundary conditions (see Figs. 2, 10 and Tables I, III). The cell has the same vertical extent as it has in radius (see [15]).

As all our figures demonstrate, the influence of strong magnetic fields on turbulence consists of suppression and deformation. The deformation consists of a prolongation of the cell structure in the vertical direction ([16]) so that δz is expected to become larger and larger (the wave number becomes smaller and smaller) for increasing magnetic field. This is true for Pr~ 1, but for smaller Pr the vertical cell size has a minimum for an intermediate value of the magnetic field (see Figs. 3 and Table I).

The cell size is minimum for the critical Reynolds number for all calculated examples of hydrodynamically stable flows with a conducting boundary (see, e.g., Figs. 5, 6, 8, and 9). This is not true, however, for containers with insulating walls for which the cell size grows with increasing magnetic field. For experiments with the critical Reynolds numbers the vertical cell size is generally two to three times larger than the radial one. The dependence of the vertical cell size on the magnetic Prandtl number is illustrated in Fig. 14. The smaller the magnetic Prandtl number the bigger are the cells in the vertical direction.

The influence of boundary conditions on the cell size disappears for wide gaps between the cylinders. For the small

TABLE III. Insulating walls: Minimum Reynolds numbers and related wave numbers for a flow with outer cylinder at rest ($\hat{\mu}=0$).

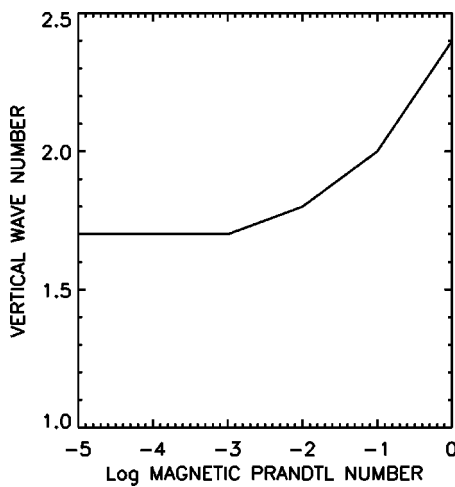| $\hat{\eta}$	Pr	Ha	Re	k
0.95	10^{-5}	0.0	185	13.6
0.95	10^{-5}	20	254	12.3
0.95	10^{-5}	40	427	8.2
0.95	10^{-5}	60	635	5.2
0.95	10^{-5}	80	846	3.8
0.95	10^{-5}	100	1058	3.0

FIG. 14. The same as in Fig. 7 but for the vertical wave number.

and medium gap, however, one finds the cells vertically more elongated for containers with insulating walls.

VI. DISCUSSION

We have shown how the MRI works in Taylor-Couette flow experiments for fluids with high and low electrical conductivity and for conducting walls as well as for insulating ones. For given microscopic viscosity the electrical conductivity determines the magnetic Prandtl number which, in the present paper, is varied from 1 to 10^{-5}. The MRI is characterized by a clear minimum in Reynolds number for a certain (critical) magnetic field strength (or Hartmann number).

However, there are drastic differences between hydrodynamically stable and unstable flows. For hydrodynamically unstable flows the minimum exists for $Pr > Pr_{min}$, where

Pr_{min} is given by Eq. (15). The Pr_{min} is of the order of unity. This means that the MRI cannot be observed in real laboratory conditions ($Pr \lesssim 10^{-5}$).

If the outer cylinder rotates so fast that the flow is hydrodynamically stable ($\hat{\mu} > \hat{\eta}^2$), the minimum Reynolds number always exists for some magnetic field strength. The coordinates of the minima depend strongly on the magnetic Prandtl number Pr. The critical Reynolds number scales as $1/Pr$ [17,18] with the magnetic Prandtl number and the critical Hartmann number scales as $1/\sqrt{Pr}$ for small Pr (see Fig. 7). Therefore, for sufficiently small values of Pr, both the critical magnetic Reynolds number Rm and the critical Lundquist number Ha* hardly depend on the magnetic Prandtl number. Thus, for hydrodynamically stable flows with small Pr, the critical numbers are almost independent of viscosity.

From Eq. (20) with $\nu = 10^{-2}$ cm²/s, $\hat{\eta} = 0.5$, and Re $\simeq 2.1 \times 10^6$ for $Pr = 10^{-5}$ and $\hat{\mu} = 0.33$ (see Fig. 6) follows

$$f = \frac{135}{(R_{out}/10 \text{ cm})^2} \quad \text{Hz} \tag{25}$$

for the frequency of the inner cylinder. Hence, a container with an outer radius of 30 cm and an inner radius of 15 cm requires a rotation of about 15 Hz in order to exhibit the MRI for liquid sodium with its magnetic Prandtl number of 10^{-5}. Following Eq. (19) the required magnetic field is about 900 Gauss.

The MRI has only been considered for axisymmetric disturbances. According to the results for small gap and small Pr (cf. [19]), the nonaxisymmetric disturbances might be more unstable for small magnetic fields. The influence of nonaxisymmetric disturbances on the MRI will be considered in a forthcoming paper.

[1] E.P. Velikhov, Sov. Phys. JETP **9**, 995 (1959).
[2] S. Chandrasekhar, *Hydrodynamic and Hydromagnetic Stability* (Clarendon, Oxford, 1961).
[3] S.A. Balbus and J.F. Hawley, Astrophys. J. **376**, 214 (1991).
[4] R.J. Donnelly and M. Ozima, Phys. Rev. Lett. **4**, 497 (1960).
[5] R.J. Donnelly and M. Ozima, Proc. R. Soc. London, Ser. A **266**, 272 (1962).
[6] R.J. Donnelly and D.R. Caldwell, J. Fluid Mech. **19**, 257 (1964).
[7] A. Brahme, Phys. Scr. **2**, 108 (1970).
[8] H. Ji, J. Goodman, and A. Kageyama, Mon. Not. R. Astron. Soc. **325**, 1 (2001).
[9] J. Goodman and H. Ji, J. Fluid Mech. **462**, 365 (2002).
[10] T. Chang and W. Sartory, Proc. R. Soc. London, Ser. A **301**, 451 (1967).

[11] This is very close to the parameters of the experiments in [14].
[12] D. Richard and J.-P. Zahn, Astron. Astrophys. **347**, 734 (1999).
[13] This assumes that there is no nonlinear hydrodynamic instability at that (high) Reynolds number [12].
[14] D.P. Lathrop, J. Fineberg and H.L. Swinney, Phys. Rev. Lett. **68**, 1515 (1992).
[15] E. L. Koschmieder, *Bénard Cells and Taylor Vortices* (Cambridge University Press, Cambridge, 1993).
[16] G. Rüdiger, Astron. Nachr. **295**, 275 (1974).
[17] G. Rüdiger and Y. Zhang, Astron. Astrophys. **378**, 302 (2001)
[18] The power-law index (here -1) is stronger than the value (-0.65) that has been found for a finite cylinder with pseudo-vacuum boundary conditions and an aspect ratio of 10 (cf. [17]).
[19] C.-K. Chen and M. Chang, J. Fluid Mech. **366**, 135 (1998).